ResearchGate

See discussions, stats, and author profiles for this publication at: https://www.researchgate.net/publication/263953949

Design of Organic Chromophores for All-Optical Signal Processing Applications

ARTICLE *in* CHEMISTRY OF MATERIALS · SEPTEMBER 2013

Impact Factor: 8.35 · DOI: 10.1021/cm402893s

CITATIONS
18

READS
74

7 AUTHORS, INCLUDING:

Joel M Hales
Georgia Institute of Technology
110 PUBLICATIONS **1,999** CITATIONS

SEE PROFILE

Stephen Barlow
Georgia Institute of Technology
285 PUBLICATIONS **11,511** CITATIONS

SEE PROFILE

Sukrit Mukhopadhyay
Georgia Institute of Technology
20 PUBLICATIONS **163** CITATIONS

SEE PROFILE

Joseph W. Perry
Georgia Institute of Technology
321 PUBLICATIONS **12,198** CITATIONS

SEE PROFILE

Available from: Seth Marder
Retrieved on: 02 February 2016

CHEMISTRY OF MATERIALS

Perspective

pubs.acs.org/cm

Design of Organic Chromophores for All-Optical Signal Processing Applications

Joel M. Hales,* Stephen Barlow, Hyeongeu Kim, Sukrit Mukhopadhyay, Jean-Luc Brédas, Joseph W. Perry,* and Seth R. Marder*

School of Chemistry and Biochemistry and Center for Organic Photonics and Electronics, Georgia Institute of Technology, Atlanta, Georgia 30332-0400, United States

ABSTRACT: Organic materials possess many key attributes that make them suitable for exploitation in all-optical signal processing applications including facile tunability of their optical properties, strong and ultrafast nonlinear optical response, and potential for integration into device structures. In this perspective, we present molecular design guidelines for organic chromophores that could serve as the active constituents for such materials. Using a relatively simple model, a candidate class of chromophores, namely cyanine-like polymethines, is identified based on promising microscopic nonlinear optical properties in the near-IR spectral region. The challenges associated with translating these microscopic properties into materials with macroscopic properties suitable for device applications are presented along with molecular engineering approaches for overcoming these hurdles.

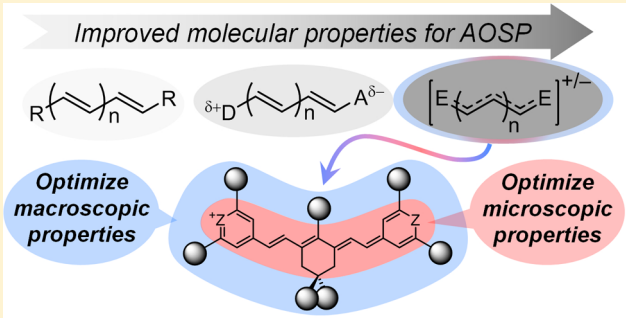

KEYWORDS: *polymethines, cyanines, polyenes, nonlinear optical materials, all-optical signal processing, all-optical switching, silicon-organic hybrids*

1. INTRODUCTION

The capacity for transmitting information, i.e. bandwidth, is increasing at an exponential rate in order to support such data-intensive areas as music and video streaming, the monitoring of market dynamics and weather patterns, telesurgery, and remote learning. Using fiber-optic cables to transmit this information using light has been quite a successful approach to accommodating this bandwidth. However, when information needs to be transferred between fibers ("fiber-to-fiber"), between computers ("chip-to-chip"), or from processor to memory on a single computer ("on-chip"), there is a bottleneck. In these cases, electronics has long been used to route and process information but may not be able to support increasingly high bandwidth demands. Furthermore, the need to convert information between the optical and electrical domains adds unwanted delays and power consumption. The ability to transmit and process information solely in the optical domain could help overcome these issues.[1]

The information carried by the light is typically transmitted along an optical waveguide (i.e., optical fiber) made of a "passive" material. The optical properties of the passive material do not change significantly as light is transmitted through it and similarly the properties of light (e.g., frequency, amplitude, phase) are largely unchanged as they pass through the material. However, optical routing, switching, or processing requires "active" nonlinear optical (NLO) materials, the optical properties of which can be modified by application of intense electromagnetic fields (such as those associated with a laser). For third-order NLO materials (see section 3) in particular, these optical properties can, in turn, be used to control the phase, amplitude, direction, polarization state, or frequency of the incident light.[2,3] Consequently, a high-intensity light beam can be used to route, switch, or modulate a signal light beam directly; these operations are generally referred to as all-optical signal processing (AOSP).

Organic materials with extensive π-systems such as polyenes, polydiacetylenes, and other conjugated polymers were identified as potential candidates for AOSP early in the history of third-order NLO materials,[4−7] but their utility was limited by various issues (see section 2). One particularly difficult hurdle to overcome was the need for the materials to function as both the active NLO material and the passive waveguide material for guiding light, which served to increase material design complexity. Over the past ten years there have been numerous efforts to exploit silicon as an active NLO material for AOSP, leading to the field of silicon nanophotonics.[8−11] While silicon is very effective at guiding light at the nanoscale, its NLO response can be compromised by a deleterious NLO effect, namely two-photon absorption (2PA). Recently, efforts aimed at combining the waveguiding properties of silicon with the tailored NLO response of organic materials in so-called silicon−organic hybrid

Special Issue: Celebrating Twenty-Five Years of Chemistry of Materials

Received: August 28, 2013
Published: September 17, 2013

 © 2013 American Chemical Society

(SOH) devices have created a resurgence in the field of organic NLO materials for AOSP.[12−15] An illustration of how a hybrid device could perform AOSP is shown in Figure 1. Here, the input

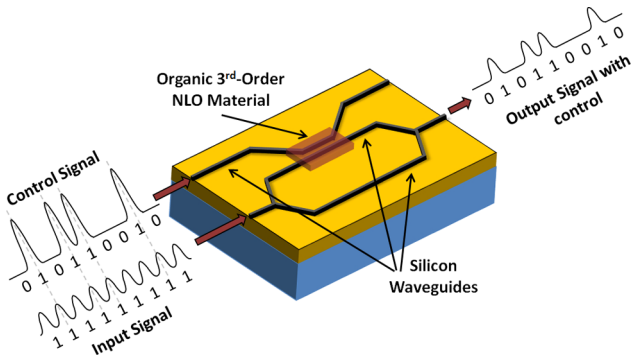

Figure 1. Illustration of AOSP using a Mach−Zehnder configuration in a silicon−organic hybrid device.

optical signal passes through an interferometric device (in a Mach−Zehnder geometry) made up of silicon waveguides. In the absence of any control signal, the input signal experiences destructive interference and no output occurs. However, when a high-intensity optical control signal is applied, changes in the optical properties of the organic NLO material lead to an alteration of the optical phase of the signal beam. This causes constructive interference, thereby enabling all-optical modulation of the input signal. Clearly the NLO properties of the organic material are critical to the efficient functioning of such devices.

In this perspective, we will present our views on molecular engineering approaches toward the development of organic materials for AOSP. We begin by outlining the various property requirements for organic materials that are needed for effective performance in SOH or other waveguide devices. We then briefly summarize the history of salient organic third-order NLO materials and discuss the potential benefits of using discrete molecular materials over polymeric ones. A framework for understanding the structure−property relationships of the microscopic third-order polarizability is presented; this framework enables identification of molecules that possess both large nonlinearities and small 2PA in the near-IR spectral region, attributes critical for AOSP. We then focus on a class of chromophores with promising molecular properties, namely polymethines, along with methods to translate these microscopic properties into macroscopic bulk materials suitable for device applications. Finally, we provide a perspective on the progress to date and the challenges that remain to be addressed.

2. MOLECULAR AND MATERIAL REQUIREMENTS FOR AOSP

In order for molecules and materials to perform effectively in AOSP, a number of properties and characteristics must be attained simultaneously. (i) Large microscopic third-order polarizabilities, γ, at wavelengths used for optical telecommunications are critical. Generally, this requires molecular structures with extended π-electron delocalization as discussed below. (ii) Ultrafast NLO response is essential for high bandwidth AOSP, as the ability to process or switch optical information requires the time scale of the nonlinear response to be shorter than the duration of the optical bits (typically <1 ps). By virtue of the electronic origin of the nonlinearity in organics, this temporal response criterion is often automatically met. (iii) Low linear and nonlinear optical losses, associated with absorption and/or scattering, are needed to avoid attenuation of the optical signal that carries information. These optical losses can also attenuate the control beam that is used to modulate or route the signal beam, reducing the overall efficiency in switching. The most significant losses generally arise from electronic absorption in the form of one-photon and two-photon absorption. (iv) The ability to retain promising microscopic properties in macroscopic materials with high molecular number density is a major goal in the development of molecular-based NLO materials. The performance of a device, such as the one shown in Figure 1,

Chart 1. Schematic Showing Some of the Structural Features of Polymethine Dyes That Can Be Varied and How They Can Affect the Material's Properties

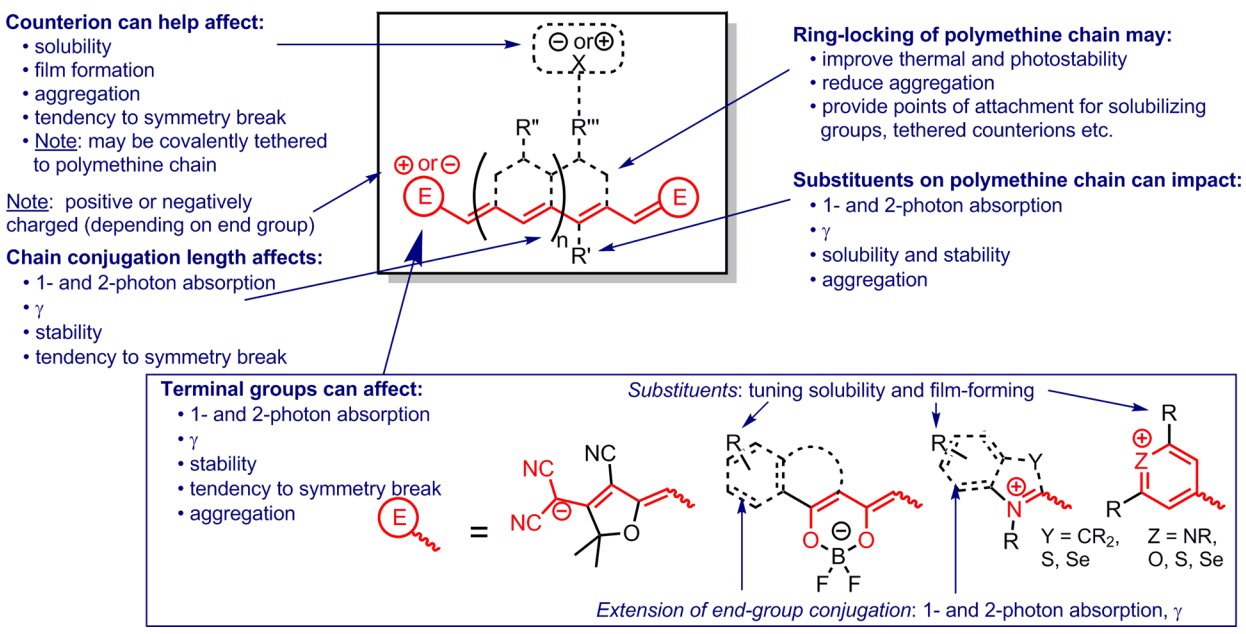

depends critically on the organic material possessing a large magnitude of the macroscopic third-order susceptibility, $|\chi^{(3)}|$, which is responsible for changes in the refractive index induced by the control beam. The value of $\chi^{(3)}$ is proportional to $\langle\gamma\rangle \times N$, where $\langle\gamma\rangle$ is the orientational average of γ (accounting for the angular distribution of the constituent molecules) and N is the molecular number density. It can be seen that a high number density of large-γ molecules is essential to obtain a large value of $\chi^{(3)}$. However, intermolecular electronic interactions (i.e., aggregation) at such high number densities can lead to substantial changes in the effective $\langle\gamma\rangle$. Therefore, the design of molecules must take into account structural features that prevent the occurrence of such effects. (v) The processability of the resulting high number-density organic materials is also critical for the infiltration of these materials into potential device structures.

One of the key benefits of employing organic materials is that their chemical and physical properties can be tailored through specific and well-defined synthetic modifications of the molecular structures. Properties that can be rationally controlled include the strengths and positions of the low-energy one-photon and two-photon electronic resonances, the nonlinear polarizabilities, the solubility, the propensity toward aggregation, compatibility with various polymer host materials, the strength of ion-pairing interactions in the case of molecular salts dissolved in solution or polymer hosts, and the photochemical and thermal stability of the NLO molecules. As an example of the flexibility that molecular engineering can afford, Chart 1 depicts a generic polymethine molecule with a myriad of structural features that can be introduced along with the impacts they can have on the resulting physical and/or optical properties at the microscopic and macroscopic levels.

In the early days of organic nonlinear optics, there was a significant emphasis on the third-order NLO response of conjugated polymers, especially polyacetylene, polydiacetylenes, polyarylenes, polyarylene vinylenes, but also rigid-rod and ladder polymers.[16−18] While large values of $\chi^{(3)}$ were realized for a number of these polymeric systems, the application of these polymers for AOSP was hampered by the presence of 2PA resonances across a large portion of the telecommunications wavelength range. In general, the ability to control the positions of the 2PA bands in conjugated polymers with low energy absorptions was rather limited, as they have many closely spaced low-lying electronic excited states. An exceptional case was that of the poly(hexa-2,4-diyne-1,6-diyl bis(*para*-toluenesulfonate)) which can be prepared in the form of single crystals.[19] For this polymer, a large nonlinear refractive index (n_2, which is proportional to the real part of $\chi^{(3)}$, see section 3.1) was observed in single-crystal channel waveguides. Subsequently, Stegeman and co-workers examined both the nonlinear refractive index and the 2PA in the telecommunications spectral region and found that the n_2 was reasonably large and the 2PA coefficient (proportional to the imaginary part of $\chi^{(3)}$; see section 3.1) was small at 1600 nm.[6] This combination would be suitable for AOSP but the utilization of this material was limited by the difficulty in processing these polymeric single-crystal waveguides into device structure.

More recently, researchers have focused on SOH device structures into which organic NLO materials have been introduced by evaporative deposition of discrete chromophore molecules[12] or by spin-coating of guest−host blends of discrete chromophoric molecules in highly processable, low optical-loss polymers.[14,15] The guest−host blend approach allows one to employ molecular engineering strategies for discrete molecules to optimize the optical properties, solubility, compatibility, etc. of discrete molecules, while taking advantage of a processable host polymer for integration into devices. This is the context for the following discussions of organic NLO materials, which include identifying classes of molecules that possess large third-order microscopic nonlinearities and molecular design approaches for avoiding interactions at high number densities that are deleterious to the macroscopic nonlinearities and optical losses.

3. IMPACT OF MOLECULAR STRUCTURE ON THIRD-ORDER NONLINEAR OPTICAL RESPONSE

3.1. Microscopic Polarizability and Simplified SOS Approach. According to eq 1, the dipole moment of a molecule as a function of electric field can be expressed in terms of the zero-field dipole moment, the linearly induced dipole, which is dependent on the electric field and the linear polarizability, and nonlinearly induced dipoles, which depend on higher order polarizabilities.

$$\mu = \mu_0 + \alpha E + \beta E^2 + \gamma E^3 + \ldots \tag{1}$$

The fourth term in the expansion, which includes the third-order microscopic polarizability, γ, is responsible for enabling the AOSP applications discussed above. Since E^2 is proportional to the intensity of the light, one can view γE^2 as an intensity-dependent response that modifies the third electric field, similar to the phenomenon described in Figure 1.

Perturbation theory allows one to express linear and nonlinear polarizabilities in terms of the relationships between the ground and excited states in what are commonly referred to as sum-over-states (SOS) expressions. Such expressions can help elucidate molecular structure−optical property relations and identify suitable candidates for applications, as detailed in section 3.2. In order to make such an analysis more tractable, the full SOS expression[20] is often truncated to include only terms with the strongest resonant denominators[21−23] and to reflect the appropriate number of excited states[23−27] dominating the response. The relevant expression for AOSP of the type represented schematically in Figure 1 is[28,29]

$$\gamma(\omega;\,\omega,\,-\omega,\,\omega) = \left(\frac{1}{5}\right)\cdot\left(\frac{1}{6}\right)\cdot\left(\frac{1}{\varepsilon_0}\right)\cdot 2\cdot\ldots \left\{\begin{aligned} &\left[\frac{\mu_{ge}{}^2\Delta\mu_{ge}{}^2}{(\Omega_{ge}-\hbar\omega)^2(\Omega_{ge}-2\hbar\omega)} + \frac{\mu_{ge}{}^2\Delta\mu_{ge}{}^2}{(\Omega_{ge}^*-\hbar\omega)(\Omega_{ge}-2\hbar\omega)(\Omega_{ge}-\hbar\omega)}\right] \\ &+ \sum_{e'}\left[\frac{\mu_{ge}{}^2\mu_{ee'}{}^2}{(\Omega_{ge}-\hbar\omega)^2(\Omega_{ge'}-2\hbar\omega)} + \frac{\mu_{ge}{}^2\mu_{ee'}{}^2}{(\Omega_{ge}^*-\hbar\omega)(\Omega_{ge'}-2\hbar\omega)(\Omega_{ge}-\hbar\omega)}\right] \\ &- \left[\frac{\mu_{ge}{}^4}{(\Omega_{ge}-\hbar\omega)^3} + \frac{\mu_{ge}{}^4}{(\Omega_{ge}^*-\hbar\omega)(\Omega_{ge}-\hbar\omega)^2}\right] \end{aligned}\right\} \tag{2}$$

where g, e, and e′ subscripts refer to the ground, first excited, and higher-lying excited states, respectively, $\Omega = (E - i\Gamma)$ where E is the energy difference between a pair of states and Γ is the

corresponding damping factor (half width of transition energy at half-maximum),[30,31] μ is the transition dipole moment, $\Delta\mu$ is the difference in state dipole moments, and $\hbar\omega$ is the photon energy. The factor of 1/5 accounts for the orientational averaging of γ for an isotropic sample while the factor of 1/6 results from the choice of expressing the induced dipole moment (the value discussed in the original SOS formalism[20]) using a power series expansion notation, as in eq 1. Finally, ε_0 is the permittivity of free space such that the input values (i.e., $\hbar\omega$, E, μ, etc.) are entered in MKS units[32] resulting in γ in units of $m^5 \cdot V^{-2}$.

The first term in eq 2 is often referred to as a "D" (dipolar) term, since only polar molecules can exhibit the nonzero values of $\Delta\mu_{ge}$ required to obtain a nonzero contribution from this term. The second group of terms are called "T" (two-photon) terms, since in a centrosymmetric system nonzero values of both μ_{ge} and $\mu_{ee'}$ imply e′ is of the same parity as g and, hence, two-photon allowed and one-photon forbidden with respect to the ground state. Finally, the last term is known as an "N" (negative) term. In principle, a *sum-over-states*, considering the contributions of all excited states, is required to give the value of γ; however, due to appearance of the square or cube of the excited state energy, E_{ge}, in the denominator of each term, the contributions of higher lying terms are generally relatively small and so much can be understood by considering only the first excited state. Moreover, the sum of T-terms is often truncated to consider only the lowest energy excited state(s) e′ with strong coupling to the first excited state e.

From eq 2 it is clear that γ (ω; ω, $-\omega$, ω), and, therefore, also the corresponding materials parameter, $\chi^{(3)}(\omega; \omega, -\omega, \omega)$, are *frequency-dependent* and *complex* quantities.[23,33] It is the real part that is directly related to the intensity-dependence of the refractive index required for AOSP.[33] Depending on the interplay of the different terms in eq 2, Re(γ) can be positive (meaning the refractive index increases with increasing intensity) or negative (index decreases with increasing intensity); either, however, can be exploited for AOSP, where the only requirement is a strong dependence of index on intensity (large |Re(γ)|). The imaginary parts of the polarizability and susceptibility, Im(γ) and Im($\chi^{(3)}$) respectively, are due to 2PA at the frequency in question.[33] As noted above, 2PA is undesirable for AOSP and should be minimized at the wavelength of interest. Consequently, one can define a 2PA figure-of-merit (2PA-FOM) that should be met in order to ensure that certain AOSP applications are feasible.[34,35] At the molecular level, this implies that |Re(γ)/Im(γ)| > 12.[28]

Equation 2 also indicates that the magnitudes of the individual D, T, and N terms, and, therefore, the possibility for achieving an overall net value of |Re(γ)|, will be largest when there are strongly one-photon-allowed (large μ_{ge}) low-lying electronic states (small E_{ge}) in the molecule. For organic π-conjugated chromophores, therefore, candidate materials of interest typically exhibit extended conjugation and/or charge-transfer-type (i.e., large $\Delta\mu_{ge}$) absorptions, as will be seen in more detail in the following section. Furthermore, the frequency dependence means that |Re(γ)| is increased at photon energies that approach one- or two-photon resonances. This *frequency dispersion* of γ is discussed in more detail in the following section and can be exploited by choosing a material and photon energy to take advantage of *near-resonance* enhancement of |Re(γ)|, while at the same time retaining a sufficiently large detuning between the photon energy and the transition energy to prevent significant one- or two-photon absorption losses.

3.2. Nonlinear Optical Response of Various Molecular Classes. The simplified SOS expression can be remarkably instructive when it comes to identifying candidate molecular materials for AOSP, particularly given the strong electronic-geometric structural correlations found for π-conjugated chromophores.[36−38] For example, in simple donor−acceptor polymethine or polyene molecules, the extent of a molecule's polarization can be related to its degree of bond-order alternation (BOA), i.e. the average difference in π-bond orders between adjacent carbon−carbon bonds along the conjugated bridge (which is directly related to the bond-length alternation). When the molecule is not significantly polarized in the ground state, it exhibits a large negative BOA (∼−0.5), whereas a strongly polarized polyene, whose structure is well-described by a zwitterionic resonance structure, possesses a large positive BOA (∼0.5). In the "cyanine" limit, where these neutral and charge-separated resonance structures make equal contributions to the ground state, the BOA approaches zero. This extent of ground-state polarization can be tuned through a number of means including the strength of the donor and/or acceptor, the topology of the π-conjugated bridge, or the reaction field induced by the medium.

Through a quantum-chemical computational approach, Meyers et al. showed that application of a static electric field across a simple donor−acceptor (DA) polyene molecule allowed for continuous tuning of its ground-state polarization.[36] Applying the SOS formalism allowed mapping of the evolution of static γ (i.e., $\hbar\omega \rightarrow 0$) as a function of BOA as shown in Figure 2. A

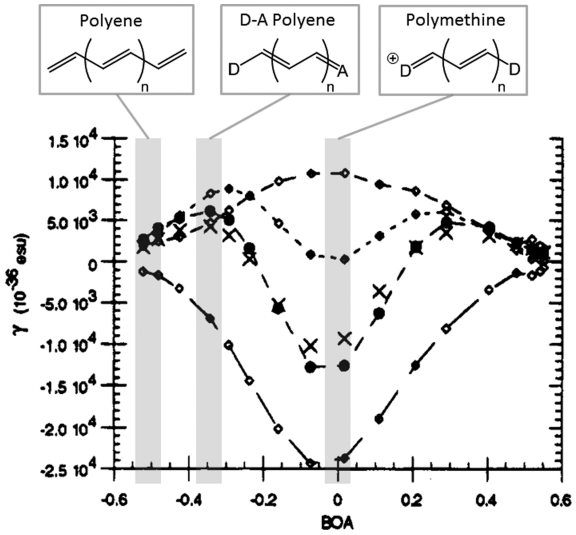

Figure 2. Evolution of static γ vs BOA for a donor−acceptor polyene for full SOS results (crosses), terms generated from truncated expression given by eq 2 as explained in text (N, diamonds/long dashed line; T, diamonds/medium dashed line; D, diamonds/short dashed line; sum of N, T, and D terms, filled circles/medium dashed line), all given in cgs units.[32] Representative molecular classes shown above graph and associated regions of BOA designated by greyed-out regions. Adapted from ref 36. Copyright 1994 American Chemical Society.

comparison of the results acquired from the full SOS calculations with those obtained from the expression given in eq 2 demonstrates the validity of using this essential-states approach. Furthermore, the inclusion of the individual D, T, and N terms illustrates their relative contributions over the various BOA regions. Several experimental studies on D−A polyenes using the

aforementioned means to tune polarization have verified this evolution of γ,[37−39] lending further credence to this approach.

A number of valuable insights for designing molecules with large NLO response can be gleaned from the evolution depicted in Figure 2. While linearly conjugated DA polyenes are an important class of chromophores, if the evolution described pertained solely to those molecules, its impact would be limited. However, similar relationships have also been reported for one-dimensional (1D) conjugated systems such as polymethines,[36,38] symmetrically substituted polyenes,[38] dipolar,[22,37,39,40] and quadrupolar[41] systems consisting of aromatic units, as well as chromophores with more pronounced 2D character.[42] Consequently, while not universally applicable, this approach can provide a good template for investigating the potential of certain molecular classes as candidates for AOSP materials. We have chosen three representative molecular classes for comparison, generic chemical structures of which are shown in Figure 2. These molecules have been chosen due to their ubiquity as NLO chromophores and the fact that they represent three distinct important BOA regions (also indicated in Figure 2). The unsubstituted polyene possesses the largest negative BOA while a dipolar DA polyene exhibits a less negative value and with appropriate donor and acceptor strength can exhibit a BOA corresponding to a positive maximum in γ. The polymethine molecule refers specifically to "cyanine-like" dyes that exhibit BOA near zero, have an odd number of carbons along the conjugated chain, and are positively or negatively charged.

The magnitude of static γ can vary quite significantly for these molecules and is dictated by the relative contributions of the T, D, and N terms. For the symmetrical polyene and polymethine molecules, the value of $\Delta\mu_{ge}$, and therefore the D term, is vanishingly small such that the sign and magnitude of γ is a result of interplay between the T and N terms. In polyenes, the first excited state is often strongly coupled to a higher lying excited state such that $\mu_{ee'}$ is large, the T term dominates, and γ is positive. However, the magnitude of γ is limited because this contribution is opposed by a substantial N term. For polymethines, γ is negative and larger in magnitude than for polyenes primarily because μ_{ge} and $1/E_{ge}$ are maximized as BOA approaches zero resulting in a substantial N term. While the N term is partially canceled by the T term, the values of $\mu_{ee'}$ for polymethines have been shown to be small, making the T term relatively small. DA polyenes in the BOA region shown in Figure 2 have substantial D term contributions, by virtue of appreciable $\Delta\mu_{ge}$ values, and, therefore, all three terms contribute significantly to the value of γ. The sign of γ is positive with a magnitude that exceeds that of an unsubstituted polyene while still falling short of that found for the polymethine.

The above discussion suggests that for molecules of comparable lengths, polymethines appear to achieve a maximal magnitude in γ. It is also instructive to examine the evolution of the nonlinearity with increasing conjugation length (L) or, equivalently, the number of π-electrons. For polymethines, it has been demonstrated that both μ_{ge} and $1/E_{ge}$ scale as L;[43] therefore, since the N term scales as $\mu_{ge}{}^4$ and $E_{ge}{}^{-3}$, the static value of γ is predicted[16] and experimentally[44,45] verified to scale as L^7. This is a decidedly more pronounced length dependence than is observed in either unsubstituted or DA polyenes ($\gamma \propto L^n$ where n = 2−4).[16,46,47] However, while long polymethines appear to be optimal structures for AOSP relative to polyenes, two important caveats must be considered. The $1/L$ dependence of E_{ge} can lead to longer conjugated polymethines having low-energy transitions with significant one-photon absorption at telecommunications wavelengths, effectively rendering them useless for AOSP. Second, a Peierls-type symmetry breaking (see section 4.1) places a practical limit on conjugation lengths for polymethine dyes. These length restrictions are not a consideration for polyenes, and since their energy gaps scale less steeply than for polymethines, one can consider using longer polyene-like molecules before one-photon absorption becomes a limiting factor. Indeed for polyacetylene, a polyene with the longest effective conjugation length, the energy gap is ∼1.5 eV,[5] well below the photon energies corresponding to telecommunications wavelengths. Nonetheless, issues associated with saturation of the NLO response with increasing chain length do exist for unsubstituted polyenes,[16,48] as manifested in a length-dependent exponent (i.e., $\gamma \propto L^{n(L)}$) that decreases with increasing length. Similarly, in DA polyenes the terminal groups become less effectively coupled to one another at longer lengths[49] leading to lower $\Delta\mu_{ge}$ values and a concomitant reduction in γ. Furthermore, the increases in both $\Delta\mu_{ge}$ and $\mu_{ee'}$ for longer conjugation lengths can lead to stronger 2PA in polyene-like molecules, an issue that becomes clearer when one looks at the dynamic response of γ.

While the evolution of static γ (i.e., $\hbar\omega \rightarrow 0$) as a function of ground-state polarization or conjugation length can be quite instructive for selecting candidate molecules, the dynamic response of γ (represented by eq 2) is needed to fully evaluate their potential. Longer conjugated systems—those likely to have a stronger nonlinear response—will possess lower energy transitions giving rise to a strong frequency dependence (dispersion) of γ in the near-IR. This dispersion can arise from near-resonance enhancement from low-lying one-photon states or through the presence of two-photon states.[23,35,50] Furthermore, it is the complex nature of γ that reveals the two critical parameters for AOSP, Re(γ), and the 2PA-FOM, defined as |Re(γ)/Im(γ)|. The dynamic response of γ can be predicted by employing a quantum-chemical computational approach to determine relevant state energies as well as state and transition dipole moments followed by application of the SOS formalism, similar to the method described above for determining static γ.[23,50] However, it is important to keep in mind that dynamic γ will be significantly more sensitive to state energies than static γ; therefore, care must be taken with quantum-chemical approaches where calculated energies may not be consistent with experimentally determined values. Fortunately, provided the appropriate state energies and dipole moments can be determined experimentally, the simplified SOS expression given by eq 2 can be used to predict the dynamic response of γ and obtain reasonably good agreement with NLO spectroscopic measurements.[28,45,51]

For the purposes of illustrating dynamic γ for our three classes of molecules, we have tabulated a representative set of their optical properties from literature reported values (see Table 1, associated energy level schematics are shown in Figure 3). The lowest energy excited states (at energy E_{01}) are one-photon allowed and were chosen to give optimal values for Re(γ) and 2PA-FOM at 1550 nm (this rationale will be explained below), a pertinent wavelength for AOSP. The properties of the polyene are reasonably representative of a larger class of molecules including polyphenylenevinylene,[52] polydiacetylene,[53] unsubstituted[54] and symmetrically substituted[55] polyenes, and stilbene-based chromophores,[56] all of which possess a second excited state at ∼1.3E_{01} that is two-photon active. The D−A polyene, by virtue of its dipolar character, possesses excited states that are both one- and two-photon allowed, i.e. at E_{01} and ∼1.6E_{01}.[22,57] The polymethine possesses a 2PA-allowed state at a relatively

Table 1. Linear and Nonlinear Optical Properties of Representative Molecular Classes[a]

	polyene	DA polyene	polymethine
E_{01}	1.39 (895)	1.24 (1000)	1.14 (1085)
E_{02}	1.80 (690)	1.98 (625)	1.25 (990)
E_{03}			1.94 (640)
$\Delta\mu_{01}$		18	
μ_{01}	12	14	19
μ_{12}	15	10	6.0
μ_{13}			1.5
Γ_{01}	0.10	0.20	0.04
Γ_{0e}	0.10	0.20	0.09
γ_{static}	5.4×10^{-35}	6.0×10^{-34}	-2.6×10^{-33}
$\mathrm{Re}(\gamma)_{1550}$	7.7×10^{-33}	-2.2×10^{-32}	-1.1×10^{-31}
$\lvert\mathrm{Re}(\gamma)/\mathrm{Im}(\gamma)\rvert$	1.0	3.7	70

[a] E values given in electronvolts (corresponding wavelength in nanometers), Γ values given in electronvolts, $\Delta\mu$ and μ values given in Debye (3.34×10^{-30} C·m), γ values given in cgs units or esu.[32]

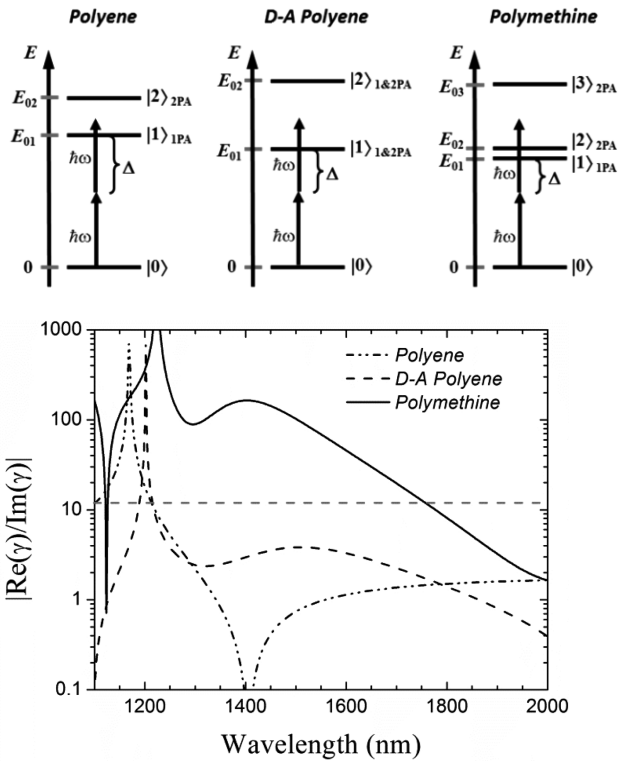

Figure 3. Energy level diagrams (top) and dispersion of 2PA-FOM (bottom) for representative molecular classes according to properties given in Table 1 and expression given in eq 2

higher energy ($\sim 1.7E_{01}$) than the polyene but also exhibits vibronically allowed 2PA in close proximity to its lowest lying excited state ($\sim 1.1E_{01}$).[28,58] While the latter activity is not strictly accounted for in the SOS analysis, it can be included heuristically using a value of $\mu_{ee'}$ that properly predicts the 2PA activity.

By employing the properties given in Table 1 along with the simplified SOS expression, both the static and dynamic values for γ (as well as the 2PA-FOM) for the various molecular systems can be determined. The static values for γ given in Table 1 illustrate that both the sign and relative magnitudes of the nonlinearities closely follow the trends predicted for the DA polyene given in Figure 2. The dynamic values for γ at 1550 nm (also given in Table 1) exhibit markedly different trends, underscoring the need to account for the frequency-dependence of the nonlinearity to accurately predict NLO responses. The most obvious consequence is the ~100× enhancement in the magnitude of the $\mathrm{Re}(\gamma)$ over static γ, primarily due to near-resonance enhancement from the lowest-lying one-photon states. This is enabled by the small detuning energies (Δ) illustrated in Figure 3 that give rise to reduced resonant denominators in eq 2 and enhanced NLO response. By virtue of nearly identical ground- and excited-state equilibrium geometries,[50,59] polymethines possess significantly narrower absorption resonances than the other molecules, as evidenced by the differences in the values for Γ in Table 1. Consequently, smaller Δ values can be achieved without experiencing linear absorption losses thereby permitting larger enhancements in $\mathrm{Re}(\gamma)$. In practice, dispersion effects due to 2PA resonances can also play a role and are partially responsible for the values of $\mathrm{Re}(\gamma)$ at 1550 nm for the polyenes, as explained below.

As mentioned, the energies of the lowest-lying states E_{01} were chosen to optimize the 2PA-FOM (i.e., $\lvert\mathrm{Re}(\gamma)/\mathrm{Im}(\gamma)\rvert$) at 1550 nm ($\hbar\omega = 0.8$ eV). As illustrated in Figure 3, this is accomplished by ensuring that $2\hbar\omega$ is sufficiently detuned from 2PA resonances and the resulting dispersion of the 2PA-FOM is shown for each of the molecules. For polyenes, there is a limit to which E_{01} can be reduced; consequently, $2\hbar\omega$ must be situated below the 2PA state at E_{02}.[54,60] While the moderate detuning energy leads to a reasonably large $\mathrm{Re}(\gamma)$, the close proximity of $2\hbar\omega$ to the strongly allowed 2PA state results in a relatively poor 2PA-FOM at 1550 nm. Furthermore, the dispersion due to the two-photon resonance gives rise to both cancellation effects in $\mathrm{Re}(\gamma)$ around 1400 nm and an enhancement in $\mathrm{Re}(\gamma)$ below the 2PA state at 1550 nm. By choosing a larger E_{01}, one can improve the 2PA-FOM considerably; however, the larger detuning energy manifests itself in a reduction in $\mathrm{Re}(\gamma)$. For DA polyenes, E_{01} is chosen such that $2\hbar\omega$ is situated between the 2PA-allowed states. While the dispersion of the 2PA-FOM exhibits a maximum around 1550 nm, it never exceeds a value of 4. This poor performance can be attributed to both strong 2PA and broad electronic transitions (i.e., Γ values of 0.2 eV) due to significant differences in ground- and excited-state geometries. Furthermore, dispersion due to the strong low-lying 2PA-allowed state is so pronounced that the $\mathrm{Re}(\gamma)$ at 1550 nm turns negative in sign, contrary to the expected positive value suggested by static γ. As for the DA polyenes, the choice of E_{01} for polymethines also places $2\hbar\omega$ between well-spaced 2PA states. However, by virtue of moderate two-photon activity and narrower linewidths, the 2PA-FOM exceeds the target value of 12 required by AOSP by a significant margin and over a broad spectral range.

To summarize, of the molecules investigated, polymethines exhibit maximal static $|\gamma|$ for a given chain length while possessing a strong power-law dependence of γ with conjugation length. Furthermore, analysis of the dynamic response of γ reveals strong near-resonance enhancement of $\mathrm{Re}(\gamma)$ and favorable values of 2PA-FOM in the telecommunications spectral region. Given these findings, the following section will focus on optimizing these promising chromophores for the development of solid-state materials suitable for AOSP device applications.

4. MOLECULAR AND MATERIALS DESIGN APPROACHES FOR POLYMETHINE CHROMOPHORES

4.1. Avoiding Symmetry Breaking in Polymethine Molecules. As discussed in the previous section, the pronounced length-dependence of γ in polymethines suggests

that extension of the bridge conjugation length could be a facile strategy for enhancing nonlinear response. However, theoretical predictions, backed up by a significant body of experimental evidence, suggest that polymethines beyond a certain critical length undergo a Peierls-type symmetry breaking wherein the charge localizes on one end of the molecule leading to significant BOA that is more reminiscent of a DA polyene.[61−65] This charge localization is deleterious as evidenced by a decrease in μ_{ge} and a concomitant increase in E_{ge} leading to an overall reduction in $|\mathrm{Re}(\gamma)|$, while the molecule can also develop strong 2PA bands. For example, pyridinium-terminated[65] and benzothiazolium-terminated[63] polymethines with 9 and 11 carbons in the central chain, respectively, both possess E_{01} values similar to the polymethine discussed in Table 1, which was calculated to exhibit such a promising NLO response. However, both systems exhibited spectroscopic signatures indicating charge localization at these conjugation lengths. Hence, one of the major challenges in exploiting polymethines for AOSP is engineering molecules with sufficiently long conjugation lengths to generate strong NLO response without succumbing to symmetry breaking.

One potential strategy to overcoming symmetry breaking is to modify the charge-stabilizing terminal groups such that they participate more efficiently in the overall conjugation length of the polymethine molecule. Terminal groups that possess good energy matching to the frontier orbitals of the conjugated bridge and provide large orbital overlap for mixing of terminal group wave functions with the π-electron wave functions of the bridge should help delocalize charge throughout the molecule and minimize the impact of charge localization.[28] A selection process that would allow for identification of terminal groups with the largest effective number of π-electrons could facilitate this search. This can be accomplished by applying a free electron model for the absorption behavior of vinylogous sets of polymethine molecules with different terminal groups. As discussed above, E_{ge} scales as $1/L$ where the effective conjugation length can be written as $L = N_\pi + 2 \times N_{term}$ with N_π being the number of π-electrons along bridge and N_{term} the effective number of π-electrons contributed by a terminal group.[65] By fitting the evolution of E_{ge} versus N_π for a variety of vinylogous polymethines (terminal groups: dimethylamino, dithiole, benthiazolium, pyridinium, thiopyrylium, selenopyrylium), the values of N_{term} were found to vary from a value of 1 for the dimethylamino groups to a value of nearly 4 for the selenopyrylium groups.[28] Furthermore, with the total effective number of delocalized π-electrons known, the progression of the lowest lying transition energies (E_{ge}) and transition dipole moments (μ_{ge}) can be plotted as a function of the effective conjugation length (see Figure 4). Among all the terminal groups, the selenopyrylium system exhibits the optimal values of E_{ge} and μ_{ge} for a given effective conjugation length.

These results indicate that the selenopyrylium group should be effective at delocalizing charge throughout the molecule. Given that this group contains the heaviest and most polarizable atom of all the heterocyclic terminals, one would expect sizable mixing of the selenium p_π orbital with the π-conjugated bridge coupled with an increase in the transition density toward the periphery of the molecule. SAC/SAC-CI quantum chemical calculations confirm this observation by revealing an appreciable electron density in the frontier orbitals of the terminal groups.[28] The efficacy of this terminal group allows one to avoid charge localization in a selenopyrylium heptamethine while achieving an E_{01} value comparable to the polymethine discussed in Table 1. Consequently, the dominance of the N term in the NLO

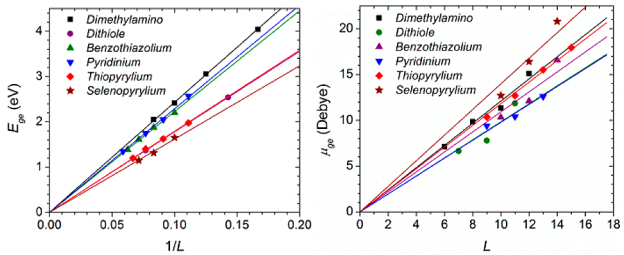

Figure 4. E_{ge} vs $1/L$ (left) and μ_{ge} vs L (right) for polymethines with various terminal groups. Reprinted from ref 28. Copyright 2010 American Association for the Advancement of Science.

response of polymethines and its steep dependence on E_{ge} and μ_{ge} gives rise to unprecedentedly large values of $|\mathrm{Re}(\gamma)|$ for this heptamethine throughout the near-IR,[28] exceeding those of other promising organic molecules including a dioxaborine (DOB)-terminated nonamethine,[66] polarized carotenoids,[67] and other DA polyenes.[68] Furthermore, the highly delocalized nature of the selenopyrylium polymethines suggests that these molecules should possess the large 2PA transparency region alluded to in the previous section. Figure 5 shows both the

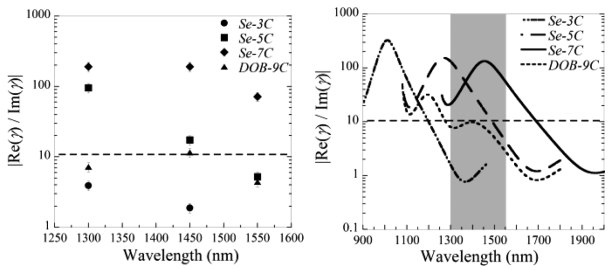

Figure 5. Dispersion of 2PA-FOM dispersion for selenopyrylium-terminated polymethines of various lengths and DOB-terminated nonamethine. Experimental data (left) and calculations from eq 2 (right). Reprinted from ref 28. Copyright 2010 American Association for the Advancement of Science.

experimentally determined and the SOS-calculated (using eq 2) 2PA-FOMs in the near-IR for the selenopyrylium-terminated polymethines of various bridge lengths. Not only are there good agreements between the plots, but the anticipated large and broadband two-photon transparency regions are clearly evident. The values of the 2PA-FOM exceed that of a promising DOB-terminated nonamethine by nearly an order-of-magnitude. Moreover, the region of transparency defined by where the 2PA-FOM exceeds the requisite value of 12 has a bandwidth of nearly 300 nm and is readily tunable by modification of the conjugated bridge length.

4.2. Design of High Number-Density Polymethine Materials. Although we have described a strategy for achieving polymethines with promising microscopic nonlinearities and FOMs, recall from section 2 that AOSP applications require materials with a large macroscopic susceptibility, $|\chi^{(3)}|$, as well as minimal linear and nonlinear optical losses. To achieve large $|\chi^{(3)}|$ in a material requires a high number density of large-$|\gamma|$ molecules, which can potentially be achieved using a concentrated solution, a neat film of chromophores, or a highly doped chromophore guest-polymer host blend. Implicit is the assumption that the optimal microscopic properties will be retained upon translation to the macroscopic material environment. However, there are two critical characteristics of cyanine-

like polymethines that should be recognized: (1) they are ions and therefore need to be associated with counterions in the solid-state to ensure overall electroneutrality, and (2) they are highly polarizable and are, therefore, prone to strong chromophore−chromophore van der Waals interactions, i.e. aggregation. As a consequence, the microscopic optical properties, which are typically measured at very low concentrations, can change dramatically when the chromophore concentration is increased due to these intermolecular interactions. Therefore, it is critical to understand the impact of chromophore−counterion interactions and chromophore−chromophore aggregation in order to design materials that will have favorable nonlinearities and FOMs in the solid state.

Effects of Counterions. Before discussing how the presence of the counterion can modify the optical properties of the chromophore, it is important to note that molecular engineering of the counterion can lead to drastic improvements in the processability of the overall complex. In solutions, by utilizing a counterion that exhibits good compatibility with the solvent environment and shows some efficacy in preventing aggregation (at least up to millimolar concentrations, see below), significant increases in concentration can be achieved. Such concentrations can facilitate synthetic chemistries, enable NLO measurements on moderately concentrated solutions for determining γ, and permit solution-based film processing such as spin-coating or drop-casting. For example, exchange of a tetrafluoroborate counterion for BAr'_4^- (Ar′ = 3,5-di(trifluoromethyl)phenyl) in a set of a thiopyrylium polymethines facilitated syntheses, NLO characterization, and processing of high number density films.[69] In solid-state films, counterion exchange has been used to significantly decrease the amount of optical scattering in guest−host systems. In the case of anionic heptamethines with tricyanofuran termini, it was found that *para*-(dimethylamino)-benzyltriphenylphosphonium counterions led to better miscibility, reduced phase segregation, and consequently reduced linear optical losses in 50:50 weight guest−host blends with an amorphous polycarbonate host when compared to other ammonium and phosphonium counterions.[14]

Often, the nature of the counterion and its interaction with the chromophore can lead to pronounced effects on the optical properties of the latter. Experimental data suggest that symmetry breaking of polymethines in solution is the result of a delicate interplay between solvent and counterion effects. For instance, in cyanine-like dyes of moderate length, dye−counterion interactions appear to be the driving force for symmetry breaking. In particular, small (and thus strongly polarizing and poorly polarizable) counterions such as halides are less able than larger ions to screen the Coulombic interactions between the dyes and their counterions, potentially leading to strong ion pairing and symmetry breaking.[62] Computational studies of the geometries of polymethine−counterion complexes can provide some insight into these trends. For shorter-chain (pentamethine) streptocyanines, the counterion is located close of the center of the polymethine bridge in the energetic minimum of an isolated dye cation and halide anion;[70,71] however, for longer chain molecules (hepta- to nonamethines), the anion is significantly displaced from a symmetrical postion and is in close proximity to one of the positively charged amino termini.[71] This ion pairing induces significant symmetry-breaking, which results in a drastic reduction of the magnitude of Re(γ). This effect can be mitigated either by utilizing a suitable dielectric medium or by using a large, less polarizing, and/or more polarizable counterion, such that interactions between the chromophore and counterion become screened.[62,71] The latter approach involving large counterions is also expected to minimize symmetry breaking through strong unsymmetrical ion pairing in solid-state films.

At the higher concentrations typically targeted for AOSP materials, the effects of these electrostatic interactions are often overwhelmed by those of strong chromophore−chromophore interactions (aggregation). This can be seen in Figure 6 where

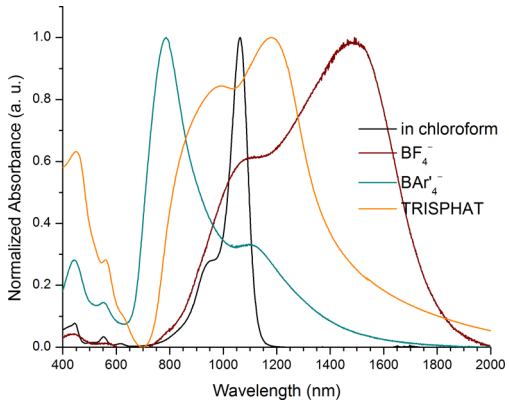

Figure 6. Absorption spectra of neat films of thiopyrylium-terminated heptamethines with various counterions including BF_4^-, BAr'_4^- {Ar′ = *m*,*m*-$(CF_3)_2C_6H_3$} and TRISPHAT {$P(o\text{-}C_6Cl_4O_2)_3^-$}. Dilute solution spectrum shown for comparison.

the neat film (i.e., 100% chromophore) absorption spectra of thiopyrylium-terminated heptamethines with different counterions are shown. Although salts with the solubilizing bulky BAr'_4^- or TRISPHAT (tris(3,4,5,6-tetrachlorobenzene-1,2-diolato)-phosphate) counterions show very different solid-state film spectra from a salt with the smaller more polarizing BF_4^- counterion, the spectra still deviate radically from the dilute solution spectrum.[72] Therefore, at high number densities, careful engineering of the counterion cannot necessarily overcome effects due to aggregation. Nonetheless, it is important to note that the molecular structure of the anion does dramatically affect the aggregation behavior and could be used as a means to control the optical properties of the resulting films.

Effects of Aggregation. In polymethines, the aforementioned intermolecular interactions can be sufficiently strong that the molecules will not only aggregate in high number-density films but even exhibit a marked tendency to aggregate in solution.[73] Many interactions can be classified as J-aggregates[74−77] or H-aggregates[78−80] based on characteristic changes in the absorption and fluorescence spectra, although perpendicular aggregates[81] and more complex structures[82−84] have also been identified. The structure of the polymethine dye itself,[83,85,86] the nature of the counterion,[87,88] and the presence of other molecular species[80,87] can affect the extent and nature of aggregation. The chalcogenopyrylium-terminated polymethines discussed above are no exception in exhibiting a strong tendency toward aggregation. Figure 6 compares the dilute solution and solid-state neat film spectra of a thiopyrylium-terminated heptamethine with the BAr'_4^- counterion. The solution spectrum reveals a strong, narrow transition in the near-IR typical of cyanine-like molecules. In more concentrated solutions (not shown)[69] relatively subtle changes in the line shape and oscillator strength are observed and attributed to interchromophore aggregation, but the film spectrum is markedly different with significant redistribution of the oscillator strength. This redistribution includes a pronounced hypsochromically shifted band around

800 nm, typically associated with H-type aggregation, which can negatively impact the film's NLO response (see below). Furthermore, there is significant bathochromically shifted absorption, possibly due to J-type aggregation, leading to unacceptable linear optical losses throughout the telecommunications region.

As well as affecting the linear absorption properties, aggregation can also adversely affect the NLO properties of the constituent chromophores.[69,74,89] Quantum-chemical investigations of the geometric and electronic structures of polymethine aggregates give insight into the possible consequences of aggregation for the optical properties of cyanine-like molecules. Pairs of streptocyanine chromophores can adopt several different structures with similar energies—J-aggregates, H-aggregates, and perpendicular structures—in all of which the electronic couplings between adjacent dye molecules lead to a splitting of the excited-state energies and the appearance of low-energy 2PA states not present for isolated molecules.[71] Along these lines, aggregation has been shown to increase the 2PA response by an order-of-magnitude, which can lead to substantial reduction in the 2PA-FOM.[74] Moreover, INDO/CI calculations on H-type, J-type, and perpendicular aggregates also corroborate experimental observations of broadening of the linear absorption spectrum of aggregates[78,88,90] (such as that observed for the heptamethine-based neat film in Figure 6). Furthermore, the negative impact of the hypsochromically shifted bands seen for H aggregates and evident in some of the experimental spectra of Figure 6 can easily be rationalized by the dominance of the N term in the NLO response of polymethines. Given the dependence of $|\mathrm{Re}(\gamma)|$ on μ_{ge}^4 and E_{ge}^{-3}, any increase in the transition energy, particularly if it is accompanied by a reduction in the transition moment, will result in a significant reduction in the NLO response.

One straightforward approach to reduce aggregation would be to dilute the chromophore concentration with an optically "innocent" material.[69,89,91] Figure 7 shows spectra of films in

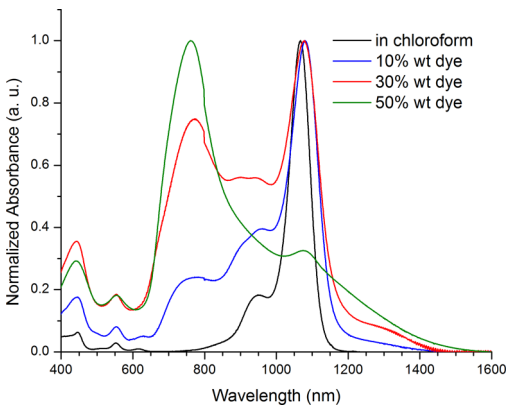

Figure 7. Absorption spectra of guest−host films of thiopyrylium-terminated heptamethine at various chromophore doping levels in amorphous polycarbonate host polymer. Dilute solution spectrum shown for comparison. Reprinted from ref 69. Copyright 2012 American Chemical Society.

which the thiopyrylium heptamethine BAr'_4^- salt of Figure 6 is diluted to varying extents by blending with an amorphous polycarbonate host polymer. Clearly, the more dilute films exhibit spectra that are considerably more solution-like than the neat film suggesting that aggregation has been reduced. Of course, the dilution necessary to disrupt aggregation also leads to a reduction in the chromophore density and in the maximum possible achievable value of $|\mathrm{Re}(\chi^{(3)})|$. More troubling is the fact that the spectra of the films with reduced chromophoric content still deviate significantly from the solution spectrum, exhibiting features similar to those observed in the neat film. Accordingly, the bathochromically shifted absorption in these films gave rise to non-negligible linear losses at 1550 nm while the hypsochromically shifted absorption is expected to lead to reduction in $|\mathrm{Re}(\chi^{(3)})|$. Interestingly, it is worth noting that aggregation effects do not necessarily lead to impaired solid-state NLO properties. For example, in the case of the promising DOB-terminated nonamethine mentioned in section 4.1, the neat-film spectrum exhibited roughly equal redistribution of the oscillator strength between the hypsochromically and bathochromically shifted bands relative to that in dilute solution.[66] Consequently, the measured values of $|\mathrm{Re}(\chi^{(3)})|$ and the 2PA-FOM were in good agreement with values extrapolated from solution, presumably due to balancing of the different contributions to $\chi^{(3)}$ from the aggregate-induced bands and to fortuitous spacing of 2PA resonances. Nonetheless, the linear losses of this film were strong in the near-IR, meaning that aggregation effects still prohibited its use in any AOSP applications.

As an alternative to the dilution approach, one could prevent the close approach of the π-systems of one dye to another by appropriate substitution of the chromophore itself.[92−95] Accordingly, we substituted thiopyrylium-terminated penta- and heptamethines with Fréchet-type dendrons.[69] As shown in Figure 8, dendronization significantly affects the spectra of neat

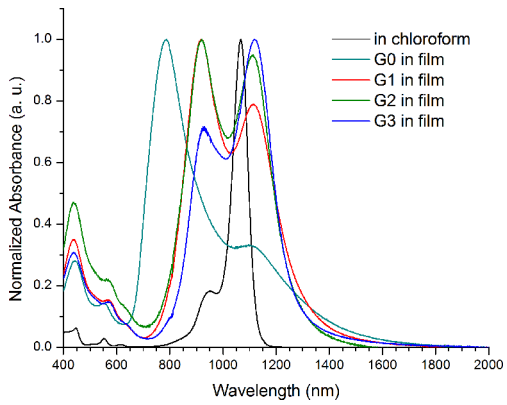

Figure 8. Absorption spectra of neat films of nondendronized (G0) and dendronized (G1−G3) thiopyrylium-terminated heptamethines. Dilute solution spectrum of G0 shown for comparison. Reprinted from ref 69. Copyright 2012 American Chemical Society.

films: for the compounds with the largest dendrons (G3 > G2 > G1), the strongest absorption peak is at least at similar energy to the solution peak. Moreover, values of $\mathrm{Re}(\chi^{(3)})$ for doped films actually approach those extrapolated from solution at chromophore loading densities higher than those for the non-dendronized chromophore (G0). However, the film spectra still differ significantly from those in solution and the films exhibited unacceptable linear losses at 1550 nm. Presumably the flexible nature of the dendrons and the groups through which they are linked to the chromophore still allow for close proximity of portions of the π-systems of neighboring dyes, thereby allowing aggregation, despite the bulkiness (and corresponding dilution effect) of the dendrons.

Another possible approach is to encapsulate the polymethine π-system within a rotaxane structure;[96,97] however, the scope of this approach is limited by synthetic considerations and the

possibility that interactions between the unencapsulated termini of the polymethines could lead to modifications of their linear and nonlinear optical properties. We believe that the most general and promising approach to achieve effective site isolation of the chromophores and ensure minimal intermolecular effects is to substitute the basic chromophore structure with relatively small (to minimize dilution effects) but rigid groups. Such groups would be chosen, for steric reasons or due to the presence of an sp^3 center immediately adjacent to the chromophore π-system, to be necessarily rigidly out-of-plane to prevent close $\pi-\pi$ approaches of neighboring chromophores. Chart 2 identifies

Chart 2. Schematic Showing Polymethines Functionalized at "Front", "End", and "Back" with Rigid Substituents

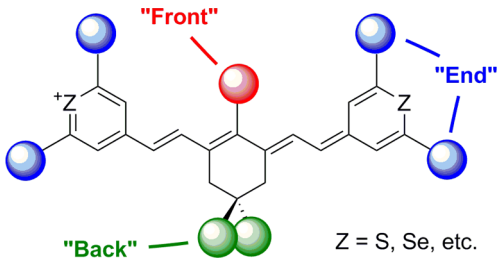

three potential classes of position in which chalcogenopyryliums can be substituted in this manner. Implementation of this strategy is currently in progress and will be reported on in an upcoming publication.

5. PERSPECTIVES AND OUTLOOK

The considerations that we have outlined above suggest cyanine-like polymethine dyes may offer the best set of properties at the molecular level among organic dyes for achieving simultaneously the large real third-order microscopic polarizabilities (i.e., $|\mathrm{Re}(\gamma)|$) and two-photon figures-of-merit (2PA-FOM, i.e. $|\mathrm{Re}(\gamma)/\mathrm{Im}(\gamma)|$) required for AOSP. This has been amply demonstrated in the case of chalcogenopyrylium substituted heptamethine dyes that exhibit exceptionally large values of $|\mathrm{Re}(\gamma)|$ and 2PA-FOM over the spectral range exploited by telecommunications. To date, attempts to develop these chromophores into high number-density materials that would exhibit the large macroscopic nonlinearities (i.e., $|\chi^{(3)}|$) needed for AOSP applications have resulted in a signification deterioration of the promising linear and nonlinear optical properties observed in dilute solution, mainly because of the strong propensity of these dyes to aggregate. However, the molecular design flexibility afforded by these polymethine chromophores provides avenues to address this issue. For example, the use of flexible-Fréchet dendrons led to a reduction in aggregation in solid-state films relative to unmodified chromophores, but this route could not eliminate the unwanted interactions. However, we believe that the use of moderately bulky substituents that are, for steric reasons, required to be rigidly out of the plane of the chromophore π-system should provide a promising pathway to overcome these aggregation issues. If such an approach can be implemented successfully, we believe that the promising microscopic nonlinearities of these polymethines will be manifest in high chromophoric-density materials with large macroscopic nonlinearities and 2PA-FOM coupled with low linear losses in the telecommunications bands. Such materials would be potentially very useful for AOSP applications and could be utilized as solid-state films in silicon–organic hybrid devices or as highly concentrated solutions in optofluidic devices such as liquid-core optical fibers. Moreover, whereas only the magnitude of the nonlinear optical response (i.e., $|\mathrm{Re}(\chi^{(3)})|$) need be large for most AOSP applications with its sign unimportant, the negative values of $\mathrm{Re}(\chi^{(3)})$ obtained for polymethine-based materials may enable them to be exploited in certain unique applications. In closing, we have outlined various strategies that may be pursued to develop molecularly based organic NLO materials for AOSP, but much work is still needed to bring the potential of these materials to realization in efficient, high-bandwidth NLO devices. We hope that this paper can inspire synthetic and materials chemists as well as materials scientists to engage in tackling these challenges that must be overcome to enable AOSP to have a dramatic impact on future high-performance telecommunications technologies.

AUTHOR INFORMATION

Notes

The authors declare no competing financial interest.

Biographies

Joseph W. Perry is a Professor in the School of Chemistry and Biochemistry at Georgia Tech. He received his B.S. in Chemistry at the University of South Florida and his Ph.D. in Chemistry at Caltech. He is a Fellow of the AAAS, APS, and OSA. His awards include a NASA Medal for Exceptional Scientific Achievement and an Invited Professorship, ENS de Lyon. He served as Topical Editor, *Journal of the Optical Society of America B*.

Seth R. Marder obtained his Ph.D. in 1985 (UW-Madison) and completed his postdoctoral research in 1987 (University of Oxford). He was a National Research Council Resident Research Associate at the Jet Propulsion Laboratory California Institute of Technology, and later joined their Technical Staff. He became a Professor of Chemistry and Optical Sciences at the University of Arizona (1998) before relocating to Georgia Tech (2003) where he is currently a Regents' Professor of Chemistry.

ACKNOWLEDGMENTS

This work was supported by the Air Force Office of Scientific Research through the COMAS MURI program (Agreement No. FA9550-10-1-0558). We also gratefully acknowledge Arpornrat Nantalaksakul for acquisition of the TRISPHAT compound neat film's linear absorption spectrum in Figure 5.

REFERENCES

(1) Ramaswami, R.; Sivarajan, K.; Sasaki, G. *Optical Networks: A Practical Perspective*, 3rd ed.; Morgan Kaufmann Publishers Inc.: New York, 2009.
(2) Asobe, M. *Opt. Fiber Technol.* **1997**, *3*, 142–148.
(3) Stegeman, G. I.; Wright, E. M.; Finlayson, N.; Zanoni, R.; Seaton, C. T. *J. Lightwave Technol.* **1988**, *6*, 953–970.
(4) Halvorson, C.; Wu, R.; Moses, D.; Wudl, F.; Heeger, A. J. *Chem. Phys. Lett.* **1993**, *212*, 85–89.
(5) Krausz, F.; Wintner, E.; Leising, G. *Phys. Rev. B* **1989**, *39*, 3701–3710.
(6) Lawrence, B. L.; Cha, M.; Kang, J. U.; Toruellas, W.; Stegeman, G.; Baker, G.; Meth, J.; Etemad, S. *Electron. Lett.* **1994**, *30*, 447–448.
(7) Stegeman, G. I.; Seaton, C. T.; Zanoni, R. *Thin Solid Films* **1987**, *152*, 231–263.
(8) Liu, X.; Driscoll, J. B.; Dadap, J. I.; Osgood, R. M.; Assefa, S.; Vlasov, Y. A.; Green, W. M. J. *Opt. Express* **2011**, *19*, 7778–7789.
(9) Osgood, J. R. M.; Panoiu, N. C.; Dadap, J. I.; Liu, X.; Chen, X.; Hsieh, I. W.; Dulkeith, E.; Green, W. M.; Vlasov, Y. A. *Adv. Opt. Photon.* **2009**, *1*, 162–235.

(10) Tanabe, T.; Notomi, M.; Mitsugi, S.; Shinya, A.; Kuramochi, E. *Opt. Lett.* **2005**, *30*, 2575−2577.
(11) Nakamura, S.; Tajima, K.; Sugimoto, Y. *Appl. Phys. Lett.* **1994**, *65*, 283−285.
(12) Koos, C.; Vorreau, P.; Vallaitis, T.; Dumon, P.; Bogaerts, W.; Baets, R.; Esembeson, B.; Biaggio, L.; Michinobu, T.; Diederich, F.; Freude, W.; Leuthold, J. *Nat. Phot.* **2009**, *3*, 216−219.
(13) Leuthold, J.; Freude, W.; Brosi, J. M.; Baets, R.; Dumon, P.; Biaggio, I.; Scimeca, M. L.; Diederich, F.; Frank, B.; Koos, C. *Proc. IEEE* **2009**, *97*, 1304−1316.
(14) Li, Z. a.; Liu, Y.; Kim, H.; Hales, J. M.; Jang, S.-H.; Luo, J.; Baehr-Jones, T.; Hochberg, M.; Marder, S. R.; Perry, J. W.; Jen, A. K.-Y. *Adv. Mater.* **2012**, *24*, 326−330.
(15) Hochberg, M.; Baehr-Jones, T.; Wang, G. X.; Shearn, M.; Harvard, K.; Luo, J. D.; Chen, B. Q.; Shi, Z. W.; Lawson, R.; Sullivan, P.; Jen, A. K. Y.; Dalton, L.; Scherer, A. *Nat. Mater.* **2006**, *5*, 703−709.
(16) Brédas, J. L.; Adant, C.; Tackx, O.; Persoons, A.; Pierce, B. M. *Chem. Rev.* **1994**, *94*, 243−278.
(17) Hales, J. M.; Perry, J. W., Organic and Polymeric 3rd-Order Nonlinear Optical Materials and Device Applications. In *Introduction to Organic Electronic and Optoelectronic Materials and Devices*; Sun, S.-S., Dalton, L., Eds.; CRC Press: Orlando, FL, 2008; pp 521−579.
(18) Luther-Davies, B.; Samoc, M. *Curr. Opin. Solid State Mater. Sci.* **1997**, *2*, 213−219.
(19) Krol, D. M.; Thakur, M. *Appl. Phys. Lett.* **1990**, *56*, 1406−1408.
(20) Orr, B. J.; Ward, J. F. *Mol. Phys.* **1971**, *20*, 513−526.
(21) Cha, M.; Torruellas, W. E.; Stegeman, G. I.; Horsthuis, W. H. G.; Mohlmann, G. R.; Meth, J. *Appl. Phys. Lett.* **1994**, *65*, 2648−2650.
(22) Kogej, T.; Beljonne, D.; Meyers, F.; Perry, J. W.; Marder, S. R.; Bredas, J. L. *Chem. Phys. Lett.* **1998**, *298*, 1−6.
(23) Kuzyk, M. G.; Singer, K. D.; Stegeman, G. I. *Adv. Opt. Phot.* **2013**, *5*, 4−82.
(24) Dixit, S. N.; Guo, D. D.; Mazumdar, S. *Phys. Rev. B* **1991**, *43*, 6781−6784.
(25) Heflin, J. R.; Wong, K. Y.; Zamanikhamiri, O.; Garito, A. F. *Phys. Rev. B* **1988**, *38*, 1573−1576.
(26) Kuzyk, M. G.; Dirk, C. W. *Phys. Rev. A* **1990**, *41*, 5098−5109.
(27) Dirk, C. W.; Cheng, L. T.; Kuzyk, M. G. *Int. J. Quantum Chem.* **1992**, *43*, 27−36.
(28) Hales, J. M.; Matichak, J.; Barlow, S.; Ohira, S.; Yesudas, K.; Brédas, J.-L.; Perry, J. W.; Marder, S. R. *Science* **2010**, *327*, 1485−1489.
(29) Butcher, P. N.; Cotter, D. *The Elements of Nonlinear Optics*; Cambridge University Press: Cambridge, 1991.
(30) Dirk, C. W.; Kuzyk, M. G. *Phys. Rev. B* **1990**, *41*, 1636−1639.
(31) The use of complex conjugates (i.e., Ω and Ω^*) in the essential states expression for eq 2 are critical for properly accounting for disperion of γ near absorption resonances, as detailed in ref 30.
(32) Conversion between the MKS units presented here and cgs units can be accomplished according to the following: γ [$m^5 \cdot V^{-2}$, MKS] = $(4\pi/9 \times 10^{-8}) \times \gamma$ [esu or $cm^5 \cdot statVolt^{-2}$, cgs].
(33) Christodoulides, D. N.; Khoo, I. C.; Salamo, G. J.; Stegeman, G. I.; Stryland, E. W. V. *Adv. Opt. Phot.* **2010**, *2*, 60−200.
(34) Mizrahi, V.; Delong, K. W.; Stegeman, G. I.; Saifi, M. A.; Andrejco, M. J. *Opt. Lett.* **1989**, *14*, 1140−1142.
(35) Stegeman, G. I. *SPIE* **1993**, *1852*, 75−89.
(36) Meyers, F.; Marder, S. R.; Pierce, B. M.; Bredas, J. L. *J. Am. Chem. Soc.* **1994**, *116*, 10703−10714.
(37) Marder, S. R.; Gorman, C. B.; Meyers, F.; Perry, J. W.; Bourhill, G.; Brédas, J.-L.; Pierce, B. M. *Science* **1994**, *265*, 632−635.
(38) Marder, S. R.; Perry, J. W.; Bourhill, G.; Gorman, C. B.; Tiemann, B. G.; Mansour, K. *Science* **1993**, *261*, 186−189.
(39) Bourhill, G.; Tiemann, B. G.; Perry, J. W.; Marder, S. R. *Nonlinear Opt.* **1995**, *10*, 49−60.
(40) Alain, V.; Redoglia, S.; Blanchard-Desce, M.; Lebus, S.; Lukaszuk, K.; Wortmann, R.; Gubler, U.; Bosshard, C.; Gunter, P. *Chem. Phys.* **1999**, *245*, 51−71.
(41) Zojer, E.; Beljonne, D.; Kogej, T.; Vogel, H.; Marder, S. R.; Perry, J. W.; Bredas, J. L. *J. Chem. Phys.* **2002**, *116*, 3646−3658.
(42) Tykwinski, R. R.; Gubler, U.; Martin, R. E.; Diederich, F.; Bosshard, C.; Gunter, P. *J. Phys. Chem. B* **1998**, *102*, 4451−4465.
(43) Kuhn, H. *J. Chem. Phys.* **1949**, *17*, 1198−1212.
(44) Hermann, J. P. *Opt. Commun.* **1974**, *12*, 102−104.
(45) Johr, T.; Werncke, W.; Pfeiffer, M.; Lau, A.; Dahne, L. *Chem. Phys. Lett.* **1995**, *246*, 521−526.
(46) Hermann, J. P.; Ducuing, J. *J. Appl. Phys.* **1974**, *45*, 5100−5102.
(47) Puccetti, G.; Blanchard-Desce, M.; Ledoux, I.; Lehn, J. M.; Zyss, J. *J. Phys. Chem.* **1993**, *97*, 9385−9391.
(48) Samuel, I. D. W.; Ledoux, I.; Dhenaut, C.; Zyss, J.; Fox, H. H.; Schrock, R. R.; Silbey, R. J. *Science* **1994**, *265*, 1070−1072.
(49) Babgi, B.; Rigamonti, L.; Cifuentes, M. P.; Corkery, T. C.; Randles, M. D.; Schwich, T.; Petrie, S.; Stranger, R.; Teshome, A.; Asselberghs, I.; Clays, K.; Samoc, M.; Humphrey, M. G. *J. Am. Chem. Soc.* **2009**, *131*, 10293−10307.
(50) Gieseking, R. L.; Mukhopadhyay, S.; Risko, C.; Marder, S. R.; Brédas, J.-L. *Adv. Mater.* **2013**, DOI: 10.1002/adma.201302676.
(51) Werncke, W.; Pfeiffer, M.; Johr, T.; Lau, A.; Grahn, W.; Johannes, H. H.; Dahne, L. *Chem. Phys.* **1997**, *216*, 337−347.
(52) Chung, S. J.; Maciel, G. S.; Pudavar, H. E.; Lin, T. C.; He, G. S.; Swiatkiewicz, J.; Prasad, P. N.; Lee, D. W.; Jin, J. I. *J. Phys. Chem. A* **2002**, *106*, 7512−7520.
(53) Polyakov, S.; Yoshino, F.; Liu, M.; Stegeman, G. *Phys. Rev. B* **2004**, *69*, 115421−1−115421−11.
(54) Shuai, Z. G.; Beljonne, D.; Bredas, J. L. *J. Chem. Phys.* **1992**, *97*, 1132−1137.
(55) Walla, P. J.; Linden, P. A.; Ohta, K.; Fleming, G. R. *J. Phys. Chem. A* **2002**, *106*, 1909−1916.
(56) Rumi, M.; Ehrlich, J. E.; Heikal, A. A.; Perry, J. W.; Barlow, S.; Hu, Z.; McCord-Maughon, D.; Parker, T. C.; Rckel, H.; Thayumanavan, S.; Marder, S. R.; Beljonne, D.; Brédas, J.-L. *J. Am. Chem. Soc.* **2000**, *122*, 9500−9510.
(57) Beverina, L.; Fu, J.; Leclercq, A.; Zojer, E.; Pacher, P.; Barlow, S.; Van Stryland, E. W.; Hagan, D. J.; Bredas, J. L.; Marder, S. R. *J. Am. Chem. Soc.* **2005**, *127*, 7282−7283.
(58) Fu, J.; Padilha, L. A.; Hagan, D. J.; Van Stryland, E. W.; Przhonska, O. V.; Bondar, M. V.; Slominsky, Y. L.; Kachkovski, A. D. *J. Opt. Soc. Am. B* **2007**, *24*, 56−66.
(59) Lu, D. Q.; Chen, G. H.; Perry, J. W.; Goddard, W. A. *J. Am. Chem. Soc.* **1994**, *116*, 10679−10685.
(60) Unsubstituted polyenes have a lowest lying 2PA state below E_{01} (see ref 54, for example), but it is weak and would only serve to further limit 2PA-FOM; consequently, it has been ignored.
(61) Barlow, S.; Henling, L. M.; Day, M. W.; Schaefer, W. P.; Green, J. C.; Hascall, T.; Marder, S. R. *J. Am. Chem. Soc.* **2002**, *124*, 6285−6296.
(62) Bouit, P.-A.; Aronica, C.; Toupet, L.; Guennic, B. L.; Andraud, C.; Maury, O. *J. Am. Chem. Soc.* **2010**, *132*, 4328−4335.
(63) Lepkowicz, R. S.; Przhonska, O. V.; Hales, J. M.; Fu, J.; Hagan, D. J.; Van Stryland, E. W.; Bondar, M. V.; Slominsky, Y. L.; Kachkovski, A. D. *Chem. Phys.* **2004**, *305*, 259−270.
(64) Przhonska, O. V.; Hu, H. H.; Webster, S.; Bricks, J. L.; Viniychuk, A. A.; Kachkovski, A. D.; Slominsky, Y. L. *Chem. Phys.* **2013**, *411*, 17−25.
(65) Tolbert, L. M.; Zhao, X. *J. Am. Chem. Soc.* **1997**, *119*, 3253−3258.
(66) Hales, J. M.; Zheng, S. J.; Barlow, S.; Marder, S. R.; Perry, J. W. *J. Am. Chem. Soc.* **2006**, *128*, 11362−11363.
(67) Marder, S. R.; Torruellas, W. E.; Blanchard-Desce, M.; Ricci, V.; Stegeman, G. I.; Gilmour, S.; Brédas, J.-L.; Li, J.; Bublitz, G. U.; Boxer, S. G. *Science* **1997**, *276*, 1233−1236.
(68) May, J. C.; Lim, J. H.; Biaggio, I.; Moonen, N. N.; Michinobu, T.; Diederich, F. *Opt. Lett.* **2005**, *30*, 3057−9.
(69) Scarpaci, A.; Nantalaksaku, A.; Hales, J. M.; Matichak, J. D.; Barlow, S.; Rumi, M.; Perry, J. W.; Marder, S. R. *Chem. Mater.* **2012**, *24*, 1606−1618.
(70) Karaman, R.; Menger, F. M. *J. Molec. Struc.: THEOCHEM* **2010**, *959*, 87−91.
(71) Mukhopadhyay, S.; Risko, C.; Marder, S. R.; Brédas, J.-L. *Chem. Sci.* **2012**, *3*, 3103−3112.
(72) It should be noted that at moderate concentrations (i.e., up to ∼5 mM), the bulky counterions do provide the beneficial effects of

increased solubility, ability to avoid symmetry-breaking, and limited aggregation.
(73) Jelley, E. E. *Nature* **1936**, *138*, 1009−1010.
(74) Belfield, K. D.; Bondar, M. V.; Hernandez, F. E.; Przhonska, O. V.; Yao, S. *Chem. Phys.* **2006**, *320*, 118−124.
(75) Busse, G.; Frederichs, B.; Petrov, N. K.; Techert, S. *Phys. Chem. Chem. Phys.* **2004**, *6*, 3309−3314.
(76) Kemnitz, K.; Yoshihara, K.; Tani, T. *J. Phys. Chem.* **1990**, *94*, 3099−3104.
(77) Tani, K.; Ito, C.; Hanawa, Y.; Uchida, M.; Otaguro, K.; Horiuchi, H.; Hiratsuka, H. *J. Phys. Chem. B* **2008**, *112*, 836−844.
(78) Baraldi, I.; Caselli, M.; Momicchioli, F.; Ponterini, G.; Vanossi, D. *Chem. Phys.* **2002**, *275*, 149−165.
(79) Caselli, M.; Latterini, L.; Ponterini, G. *Phys. Chem. Chem. Phys.* **2004**, *6*, 3857−3863.
(80) Gadde, S.; Batchelor, E. K.; Weiss, J. P.; Ling, Y.; Kaifer, A. E. *J. Am. Chem. Soc.* **2008**, *130*, 17114−17119.
(81) Etter, M. C.; Kress, R. B.; Bernstein, J.; Cash, D. J. *J. Am. Chem. Soc.* **1984**, *106*, 6921−6927.
(82) Didraga, C.; Pugzlys, A.; Hania, P. R.; von Berlepsch, H.; Duppen, K.; Knoester, J. *J. Phys. Chem. B* **2004**, *108*, 14976−14985.
(83) Mishra, A.; Behera, R. K.; Behera, P. K.; Mishra, B. K.; Behera, G. B. *Chem. Rev.* **2000**, *100*, 1973−2011.
(84) von Berlepsch, H.; Böttcher, C.; Dähne, L. *J. Phys. Chem. B* **2000**, *104*, 8792−8799.
(85) Gorner, H.; Chibisov, A. K.; Slavnova, T. D. *J. Phys. Chem. B* **2006**, *110*, 3917−3923.
(86) Kawasaki, M.; Aoyama, S.; Kozawa, E. *J. Phys. Chem. B* **2006**, *110*, 24480−24485.
(87) Batchelor, E. K.; Gadde, S.; Kaifer, A. E. *Supramol. Chem.* **2010**, *22*, 40−45.
(88) Das, S.; Bwambok, D.; El-Zahab, B.; Monk, J.; de Rooy, S. L.; Challa, S.; Li, M.; Hung, F. R.; Baker, G. A.; Warner, I. M. *Langmuir* **2010**, *26*, 12867−12876.
(89) Matsumoto, S.; Kubodera, K.; Kurihara, T.; Kaino, T. *Opt. Commun.* **1990**, *76*, 147−150.
(90) Shapovalov, S. A.; Samoilov, E. A. *Russ. Chem. Bull. Int. Ed.* **2008**, *57*, 1405−1415.
(91) Kohn, F.; Hofkens, J.; Wiesler, U. M.; Cotlet, M.; van der Auweraer, M.; Mullen, K.; De Schryver, F. C. *Chem.—Eur. J.* **2001**, *7*, 4126−33.
(92) Ma, H.; Jen, A. K. Y. *Adv. Mater.* **2001**, *13*, 1201−1205.
(93) Pollak, K. W.; Leon, J. W.; Frechet, J. M. J.; Maskus, M.; Abruna, H. D. *Chem. Mater.* **1998**, *10*, 30−38.
(94) Setayesh, S.; Grimsdale, A. C.; Weil, T.; Enkelmann, V.; Mullen, K.; Meghdadi, F.; List, E. J. W.; Leising, G. *J. Am. Chem. Soc.* **2001**, *123*, 946−953.
(95) Vogtle, F.; Gestermann, S.; Hesse, R.; Schwierz, H.; Windisch, B. *Prog. Polym. Sci.* **2000**, *25*, 987−1041.
(96) Rao, T.; Huff, J.; Bieniarz, C. *Tetrahedron* **1998**, *54*, 10627−10634.
(97) Yau, C. M. S.; Pascu, S. I.; Odom, S. A.; Warren, J. E.; Klotz, E. J. F.; Frampton, M. J.; Williams, C. C.; Coropceanu, V.; Kuimova, M. K.; Phillips, D.; Barlow, S.; Bredas, J. L.; Marder, S. R.; Millar, V.; Anderson, H. L. *Chem. Commun.* **2008**, 2897−2899.